Intramolecular Hydrogen Atom Transfer in Aminyl Radical at Room Temperature with Large Kinetic Isotope Effect

Ying Wang, Arnon Olankitwanit, Suchada Rajca, Andrzej Rajca*

Department of Chemistry, University of Nebraska, Lincoln, Nebraska 68588-0304.

Supporting Information Placeholder

ABSTRACT: We report a large kinetic isotope effect at 298 K, $k_H/k_D \approx 150$, associated with an intramolecular 1,5-hydrogen atom transfer (1,5-HAT) in the decay of PEGylated carbazyl (aminyl) radical in solution. The experimental observations surprisingly combine the hallmarks of tunneling, including large KIEs and unusual activation parameters, with linear Arrhenius and Eyring plots over an exceptionally wide temperature range of 116 K.

1,3,6,8-Tetra-*tert*-butyl carbazyl (TTBC) is one of very few nitrogen-centered (aminyl) radicals that are stable at ambient conditions and can be isolated as a solid (Figure 1).[1,2] Although this structural motif is attractive as the building block for organic magnetic materials,[3–7] TTBC has received little attention since its report by Neugebauer and Fischer in 1971.[1] With our recent development of polynitroxide scaffolds as organic radical contrast agents (ORCAs) for magnetic resonance imaging,[8] we have been exploring the feasibility of using aminyl radicals in the next generation of ORCAs. We were interested in TTBC as a framework in the design of stable, water soluble radicals. We envisioned that hydrophilic derivatives of the hydrophobic *t*-butyl groups in TTBC, as in the methoxy polyethylene glycol (mPEG) substituted **1**-H, would provide solubility in water while maintaining adequate stability.

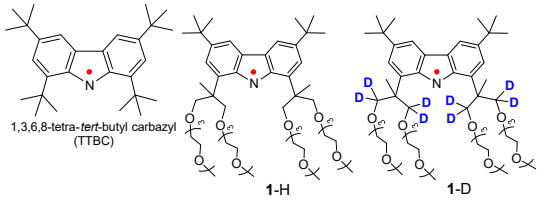

Figure 1. TTBC and aminyl radicals **1**-H and **1**-D.

We prepared radical **1**-H and found that it had a short half-life, $\tau_{1/2} \sim 1$ min, at 298 K. We suspected that an intramolecular 1,5-hydrogen atom transfer (1,5-HAT)[9–11] from the -CH_2-O- fragment[12,13] might be the factor in the short half-life of **1**-H. We investigated the D_8-isotopomer **1**-D and found that it had a much longer half-life, $\tau_{1/2} > 1$ h, with extremely large room-temperature kinetic isotope effect (KIE), e.g., $k_H/k_D \approx 150$ in acetone. This magnitude of KIE suggests the possibility of quantum mechanical tunneling (QMT),[14,15] a fascinating phenomenon. Intramolecular HAT, has been widely investigated[9–11,16] and recognized in regioselective radical C-H activation. 1,5-HAT involving nitrogen-centered radicals may be relevant to organocatalysis.[17]

Here we report the synthesis and decay kinetics of aminyl radical **1**-H and its isotopomer **1**-D.

The synthesis of **1**-H and **1**-D, starting from 1,8-dibromo-3,6-di-*tert*-butylcarbazole[18] (**2**), is outlined in Scheme 1.

Scheme 1. Synthesis of 1-H and 1-D.

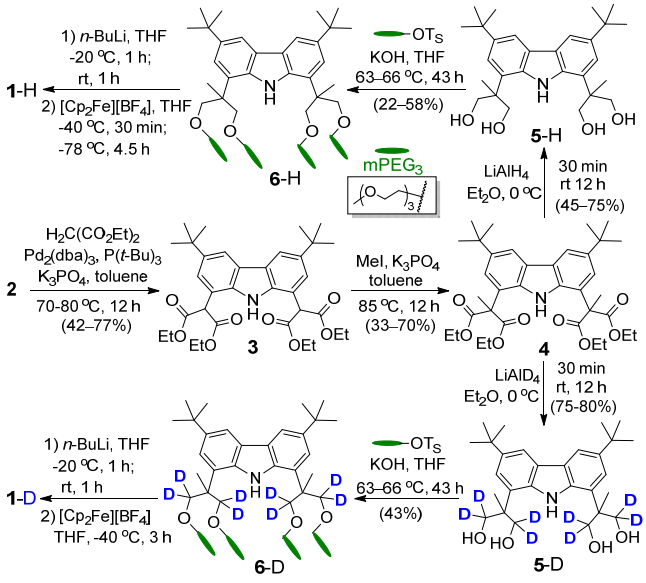

Pd-catalyzed cross-coupling of malonate with carbazole **2** afforded **3**, which was alkylated with methyl iodide[19] to provide **4**. Reduction of **4** with $LiAlH_4$ or $LiAlD_4$ afforded either **5**-H or **5**-D. Subsequent Williamson etherification gave the carbazoles **6**-H and **6**-D. ^{1}H NMR spectra indicated >99% deuteration in **6**-D. Treating **6**-H and **6**-D with *n*-BuLi, followed by one-electron oxidation of the resultant *N*-centered anion using ferrocenium cation ($[FeCp_2][BF_4]$) at low temperature provided aminyl radicals **1**-H and **1**-D. The blue solution of the radical was diluted with cold pentane and purified by column chromatography at –95 °C (for **1**-H) and –40 °C (for **1**-D) using deactivated silica gel.[20] After removal of the solvents at –40 °C, **1**-D was characterized by paramagnetic ^{1}H NMR spectroscopy,

which shows broadened peaks of **1**-D accompanied by sharp peaks of unreacted carbazole **6**-D. EPR spin counting determinations indicated spin concentration of 32–45% for **1**-H and 51–63% for **1**-D. The spin concentration of **1**-H notably correlated inversely with the length of time for removal of solvents at −40 °C. These results provide initial clues about the stabilities of **1**-H and isotopomer **1**-D.

The decays of **1**-H and **1**-D were studied by EPR spectroscopy and superconducting quantum interference device (SQUID) magnetometry. First order rate constants, k, were obtained by monitoring the decay of the mid-field EPR peak height and SQUID paramagnetic susceptibility of the aminyls. Data derived from the double integrated EPR spectra were found to produce similar values of k (see: the Supporting Information (SI)). Arithmetic means of multiple EPR measurements and, at selected temperatures, of two or more different samples were obtained to ensure reproducibility of k values. At least 10 data points were fit to the first order rate equation in each case. For **1**-H and **1**-D, k values were determined at 13 and 11 different temperatures in the 182 – 298 K and 232.5 – 316 K ranges (spanning 116 K and 93 K). The temperatures of the measurements were limited by the liquid range of solvent and decay half-lives ($\tau_{1/2}$). Long $\tau_{1/2}$ in the low temperature range, e.g., $\tau_{1/2} \approx 106$ days for **1**-D at 232.5 K, required long measurement times and good accuracy.

The kinetic observations (Table 1 and Fig. 2) have many remarkable features. The decay of **1**-H still proceeds at 182 K, indicating a low $\Delta H^{\ddagger}$ (10.0 kcal mol^{-1}) despite a calculated $\Delta H^{\ddagger}$

Table 1. Decay Kinetics of 1-H and 1-D in Acetone.[a,b]

	T (K)	E_a (kcal/mol)	ln A	$\Delta H^{\ddagger}$ (kcal/mol)	$\Delta S^{\ddagger}$ (e.u.)
1-H	182 – 298	10.5 ± 0.3	13.5 ± 0.8	10.0 ± 0.3	–33.3 ± 1.4
1-D	232 – 316	15.5 ± 0.8	17.1 ± 1.5	14.9 ± 0.8	–26.4 ± 2.9

[a] First order rate constants determined by either mid-field peak height of the EPR spectrum or paramagnetic susceptibility measured by SQUID (Fig. 2). [b] Error bars correspond to the 95% confidence intervals (Tables S5 – S10, SI).

(see below) of ≥20 kcal mol^{-1}. The KIE of ~150 at room temperature is unusually large and is one of the largest known at this temperature.[21–23] The most striking feature of the KIE, however, is the degree to which it increases at the temperature decreases. KIEs normally increase with decreasing temperature (with some interesting exceptions),[24,25] but the observed KIE here rises to ~360 at 253 K and 1380 at 232 K, far more than is consistent with an ordinary isotopic difference in activation parameters. The unusual nature of this rise is easily recognized from the Eyring plots where the slopes for **1**-H versus **1**-D differ substantially. This is reflected in the anomalously large difference in the enthalpies of activation, with $\Delta\Delta H^{\ddagger}$ = 4.90 ± 0.38 kcal mol^{-1} (mean ± SEM). Analogous anomalous values are found for Arrhenius activation energies and pre-exponential factors, i.e., $\Delta\Delta E_a$ = 4.97 ± 0.38 kcal mol^{-1} and A_H/A_D = 0.027 ± 0.020 (mean ± SEM). For reference, the difference in zero-point energy for an aliphatic C–H versus C–D stretching vibration is only ~1.1 kcal mol^{-1} and A_H/A_D should be greater than about 0.7.[26] Thus, the observed difference in the activation parameters ($\Delta\Delta H^{\ddagger}$ and $\Delta\Delta E_a$) upon isotopic substitution far exceeds the semiclassical maximum for an over-the-barrier reaction.[25,26] Unusual activation parameters have often been observed for isotope effects, and these are normally understood to be a consequence of the curvature of Arrhenius or Eyring plots.[25] However, the obtained Eyring and Arrhenius plots *are indistinguishable from linear over the broad 116 and 93 K temperature range* (Fig. 2). This is not in line with the typical signature of QMT and it is most likely indicative of thermally (vibrationally) activated tunneling,[25] e.g., analogous to that observed in 1,5-H-shift in derivatives of cyclopentadiene and *cis*-1,3-pentadiene.[27,28]

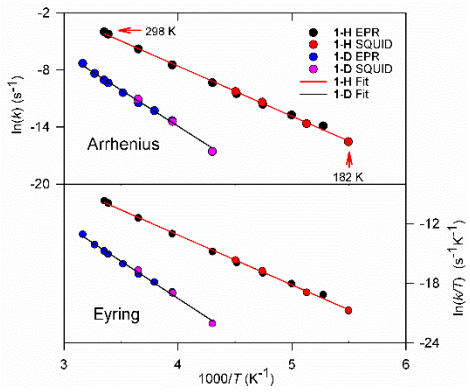

Figure 2. Decay kinetics of **1**-H and **1**-D in acetone: numerical fits to the Arrhenius (top) and Eyring (bottom) equations. The first order rate constants (k) were measured using mid-field peak height of the EPR spectrum and paramagnetic susceptibility using SQUID.

A series of experimental observations were obtained to delineate the reactions of **1**-H and **1**-D and the specific step defining the isotope effect being observed. Decay of **1**-H (32–45% spin concentration, containing **6**-H) at room temperature showed a mixture of carbazole **6**-H and aldehyde **7**-H, as indicated by ^{1}H NMR and mass spectroscopic analyses. Isolation by preparative thin layer chromatography (PTLC) provided **6**-H and the low polarity aldehyde **7**-H in 59% and 17% yields. The structure of **7**-H was confirmed using 2-D NMR spectroscopy and correlations between the DFT-calculated and experimental ^{1}H/^{13}C NMR chemical shifts. Aldehyde **7**-H is possibly the product of β-scission (fragmentation) of the C-centered radical **1**-H-C1 formed by 1,5-HAT, or more likely, of disproportionation of **1**-H-C1, followed by reaction of a product carbocation with trace amounts of water,[29] thus providing indirect evidence for the C-centered radical intermediate (Scheme 2).

For the decay of **1**-H at 253.2 K and of **1**-D at 295.2 K, first order rate constants are practically identical in acetone-h_6 and acetone-d_6 at 295.2 K, thus indicating that the solvent isotope effect is essentially negligible.[30a]

We attempted a spin trapping[31] experiment (Scheme 2). Addition of 10 equiv of *t*-BuN=O dimer (in the absence of light) does not significantly affect the rate of decay of **1**-H at 253 K.[31c] Formation of a relatively persistent nitroxide radical (g = 2.0058, a_N = 1.32 mT) was observed, and HR ESI- MS of the product **11**-H (in the mixture with **6**-H) is consistent with spin trapping of C-radical **1**-H-C1.[31]

The decay of **1**-D at room temperature provided aldehyde **7**-D (d_7-isotopomer of **7**-H) and a lower polarity minor product, which was tentatively assigned to a mixture of alkenes **8**-D and

Scheme 2. Product Analyses for the Decay of Aminyl Radicals 1-H and 1-D.

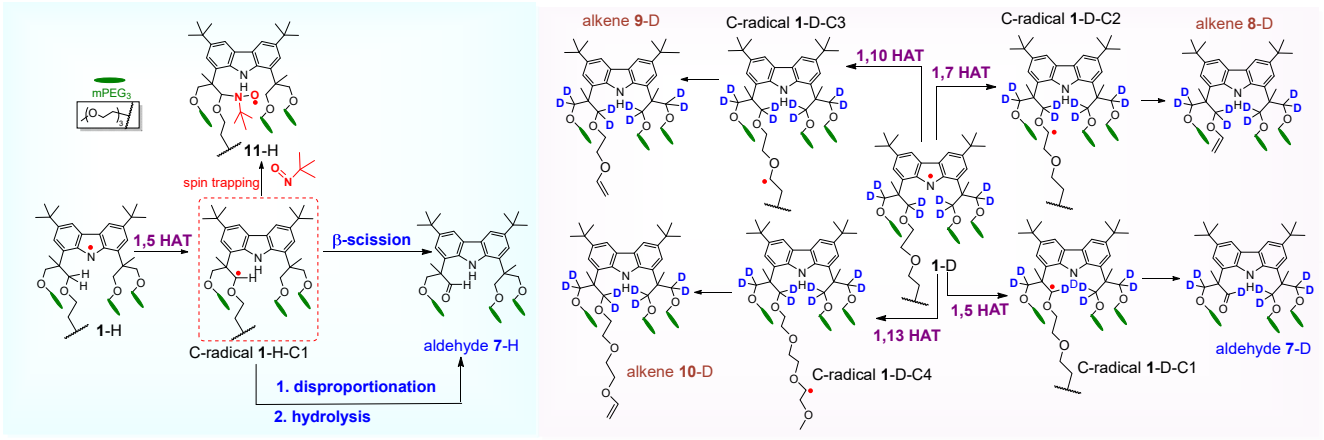

Scheme 3. UB3LYP/6-311+G(d,p)+ZPVE Energies in Acetone Using the IEF-PCM-UFF Solvent Model.

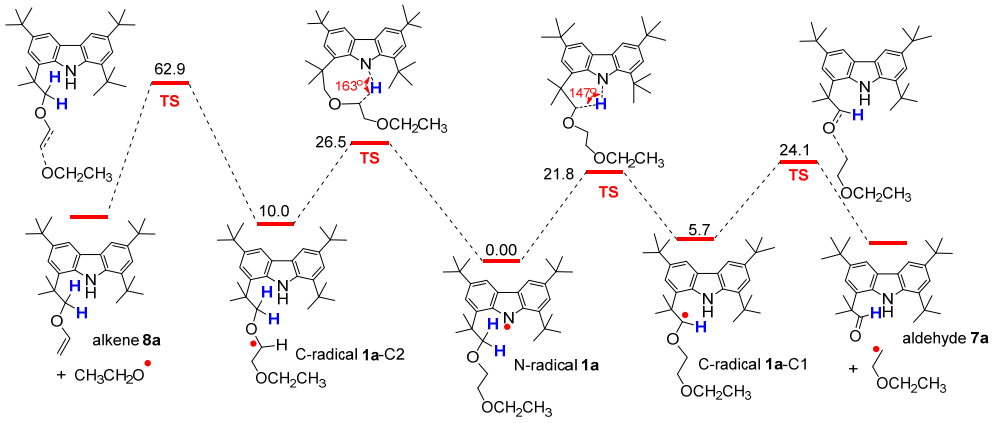

9-D (2:1 relative intensity in ESI MS). Isolated yields for **6**-D, **7**-D, **8**-D/**9**-D were 49%, 11%, and 4%; the PTLC fraction of **7**-D also contained a small amount of alkene **10**-D. In addition, a more polar fraction was isolated in 8% yield (SI). The lower yield of **7**-D, compared to **7**-H, and the formation of alkenes **8**-D – **10**-D, suggests that the decay of **1**-D includes not only the intramolecular 1,5-HAT (D-transfer) but also intermolecular or intramolecular HAT from other C-H bonds on the $mPEG_3$ chains through 8- and higher-membered TS (Scheme 2). Although the alternative HAT processes are not major, their contribution indicates that the KIEs based on the rates of decay of **1**-H and **1**-D, may be viewed as lower limits.

To support our experimental findings, we located relevant transition states on the potential energy surface (PES) of the simplified model aminyl radical **1a** (N-radical **1a**) and its decay products (Scheme 3).[32] Two transition states (TS) for intramolecular HATs from N-radical **1a** were identified. The lowest energy TS corresponded 6-membered ring with N-H-C angle of 147°, which had an activation energy, E_a = 21.8 kcal mol^{-1}, and led to C-radical **1a**-C1, which was 5.7 kcal mol^{-1} above **1a**. Another TS corresponded to 8-membered ring with N-H-C angle of 163°, which had an E_a = 26.5 kcal mol^{-1}, and led to C-radical **1a**-C2, which was 10.0 kcal mol^{-1} above **1a**. We modelled formation of aldehyde **7a** and alkene **8a** via β-scission from the corresponding C-radicals **1a**-C1 and **1a**-C2; as the relevant TS's have E_a = 24.1 and 62.9 kcal mol^{-1} (vs. **1a**), they are not likely to be significant contributors to the decay of **1**-H.

We estimated contribution of QMT to the observed KIE using UM06-2X PES[33] and asymmetric Eckart barrier for 1,5-HAT step from **1a** to **1a**-C1;[34] the computed ratios of tunneling correction factors (Γ^*_H/Γ^*_D) for **1a** and its D_2-isotopomer are 399 and 34 at 232.5 and 298 K (Table 2). If the corresponding over-the-barrier KIEs at 232.5 and 298 K are near their typical values of 8 and 5,[10c,11] then estimated $k_H/k_D \approx 3200$ and 170 (Table S14, SI) are not far off from the experimental values k_H/k_D of 1380 and 156 (Table S11 and Figure S2, SI).[35]

Table 2. Eckart-Barrier Tunneling Correction Factors (Γ^*_H and Γ^*_D) for 1,5-HAT Step.[a]

	Isotopomer	298 (K)	232.5 (K)
Γ^*_H	H_2	683.9	317077
Γ^*_D	D_2	19.9	794.4

[a] UM06-2X/6-311+G(d,p)/IEF-PCM-UFF+ZPVE PES.[33]

In summary, aminyl radical **1**-H was found to decompose via 1,5-HAT, with unusual activation parameters for isotope effects (H vs. D) and a large contribution from QMT. Nevertheless, Arrhenius and Eyring plots remain linear over a 116 K range. These unusual results may provide inspiration for theoreticians to reproduce our experimental data.[35] In particular, it would also be interesting to see whether tunneling can affect stereoselectivity of 1,5-HAT, e.g., in **1**-H, the C-H bonds of within each of methylene moieties are diastereotopic.

ASSOCIATED CONTENT

Supporting Information

General procedures and materials, additional experimental details, and complete ref 32. This material is available free of charge via the Internet at http://pubs.acs.org.

AUTHOR INFORMATION

Corresponding Author

arajca1@unl.edu

Notes

The authors declare no competing financial interests.

ACKNOWLEDGMENT

We thank the NSF (CHE-1362454 and CHE-1665256) and NIH (R01 EB-019950-01A1) for support of this research.

REFERENCES

1. Neugebauer, F. A.; Fischer, H. *Angew. Chem., Int. Ed.* **1971**, *10*, 732–733.
2. Neugebauer, F. A.; Fisher, H.; Bamberger, H.; Smith, S. O. *Chem. Ber.* **1972**, *105*, 2694–2713.
3. (a) Gallagher, N.; Olankitwanit, A.; Rajca, A. *J. Org. Chem.* **2015**, *80*, 1291–1298. (b) Rajca, A.; Olankitwanit, A.; Wang, Y.; Boratyński, P. J.; Pink, M.; Rajca, S. *J. Am. Chem. Soc.* **2013**, *135*, 18205–18215.
4. (a) Rajca, A.; Wongsriratanakul, J.; Rajca, S. *Science.* **2001**, *294*, 1503–1505. (b) Rajca, A.; Wongsriratanakul, J.; Rajca, S. *J. Am. Chem. Soc.* **2004**, *126*, 6608–6626. (c) Rajca, S.; Rajca, A.; Wongsriratanakul, J.; Butler, P.; Choi, S. *J. Am. Chem. Soc.* **2004**, *126*, 6972–6986. (d) Rajca, A.; Wongsriratanakul, J.; Rajca, S.; Cerny, R. L. *Chem. Eur. J.* **2004**, *10*, 3144–3157.
5. Ratera, I.; Veciana, J. *Chem. Soc. Rev.* **2012**, *41*, 303–349.
6. Luo, D.; Lee, S.; Zheng, B.; Sun, Z.; Zeng, W. D.; Huang, K. W.; Furukawa, K.; Kim, D.; Webster, R. D.; Wu, J. S. *Chem. Sci.* **2014**, *5*, 4944–4952.
7. Wingate, A. J.; Boudouris, B. W. *J. Polym. Sci., Part A: Polym. Chem.* **2016**, *54*, 1875–1894.
8. Rajca, A; Wang, Y.; Boska, M.; Paletta, J. T.; Olankitwanit, A.; Swanson, M. A.; Mitchell, D. G.; Eaton, S. S.; Eaton, G. R.; Rajca, S. *J. Am. Chem. Soc.* **2012**, *134*, 15724–15727.
9. (a) Nechab, M.; Mondal, S.; Bertrand, M. P. *Chem. Eur. J.* **2014**, *20*, 16034–16059. (b) Chiba, S.; Chena, H. *Org. Biomol. Chem.* **2014**, *12*, 4051–4060.
10. (a) Hofmann, A. W. *Ber. Dtsch. Chem. Ges.* **1883**, *16*, 558–560. (b) Löffler, K.; Freytag, C. *Ber. Dtsch. Chem. Ges.* **1909**, *42*, 3427–3431. (c) Corey, E. J.; Hertler, W. R. *J. Am. Chem. Soc.* **1960**, *82*, 1657–1668.
11. DeZutter, C. B.; Horner, J. H.; Newcomb, M. *J. Phys. Chem. A.* **2008**, *112*, 1891–1896.
12. Blanksby, S. J.; Ellison, G. B. *Acc. Chem. Res.* **2003**, *36*, 255–263.
13. (a) Boratynski, P. J.; Pink, M.; Rajca, S.; Rajca, A. *Angew. Chem., Int. Ed.* **2010**, *49*, 5459–5462. (b) Rajca, A.; Olankitwanit, A.; Rajca, S. *J. Am. Chem. Soc.* **2011**, *133*, 4750–4753
14. (a) Brunton, G.; Griller, D.; Barclay, L. R. C.; Ingold, K. U. *J. Am. Chem. Soc.* **1976**, *98*, 6803–6811. (b) Brunton, G.; Gray, J. A.; Griller, D.; Barclay, L. R. C.; Ingold, K. U. *J. Am. Chem. Soc.* **1978**, *100*, 4197–4200.
15. (a) Bell, R. P. *The Tunnel Effect in Chemistry*; Chapman and Hall: London-New York, 1980. (b) Ley, D.; Gerbig, D.; Schreiner, P. R. *Org. Biomol. Chem.* **2012**, *10*, 3781–3790. (c) Meisner, J.; Kästner, J. *Angew. Chem., Int. Ed.* **2016**, 55, 5400–5413.
16. (a) Pan, Z.; Horner, J. H.; Newcomb, M. *J. Am. Chem. Soc.* **2008**, *130*, 7776–7777. (b) Fukuzumi, S.; Kobayashi, T.; Suenobu, T. *J. Am. Chem. Soc.* **2010**, *132*, 1496–1497. (c) Bercaw, J. E.; Chen, G. S.; Labinger, J. A.; Lin, B. L. *J. Am. Chem. Soc.* **2008**, *130*, 17654–17655. (d) Ghosh, M.; Nikhil, Y. L. K.; Dhar, B. B.; Gupta, S. S. *Inorg. Chem.* **2015**, *54*, 11792–11798.
17. (a) Choi, G. J.; Zhu, Q.; Miller, D. C.; Gu, C. J.; Knowles, R. R. *Nature* **2016**, *539*, 268-271. (b) Studer, A.; Curran, D. P. *Angew. Chem., Int. Ed.* **2016**, 55, 58–102. (c) Jeffrey, J. L.; Terrett, J. A.; MacMillan, D. W. *Science* **2015**, *349*, 1532–1536. (d) Martínez, C.; Muñiz, K. *Angew. Chem., Int. Ed.* **2015**, *54*, 8287–8291.
18. Gibson, V. C.; Spitzmesser, S. K.; White, A. J. P.; Williams, D. J. *Dalton Trans.* **2003**, 2718–2727.
19. Beare, N. A.; Hartwig, J. F. *J. Org. Chem.* **2002**, *67*, 541–555.
20. (a) Rajca, A.; Takahashi, M.; Pink, M.; Spagnol, G.; Rajca, S. *J. Am. Chem. Soc.* **2007**, *129*, 10159–10170. (b) Vale, M.; Pink, M.; Rajca, S.; Rajca, A. *J. Org. Chem.* **2008**, *73*, 27–35.
21. Hu, S.; Sharma, S. C.; Scouras, A. D.; Soudackov, A. V.; Marcus Carr, C. A.; Hammes-Schiffer, S.; Alber, T.; Klinman, J. P. *J. Am. Chem. Soc.* **2014**, *136*, 8157–8160.
22. Huynh, M. H. V.; Meyer, T. J. *Proc. Natl. Acad. Sci. U.S.A.* **2004**, *101*, 13138–13141.
23. Huynh, M. H. V.; Meyer, T. J. *Angew. Chem. Int. Ed.* **2002**, *41*, 1395–1398.
24. Storer, J. W.; Houk, K. N. *J. Am. Chem. Soc.* **1993**, *115*, 10426–10427.
25. Kohen, A. *Prog. React. Kin. Mechanism* **2003**, 28, 119–156.
26. Kim, Y.; Kreevoy, M. M. *J. Am. Chem. Soc.* **1992**, *114*, 7116–7123.
27. (a) Roth, W. R.; König, J. *Liebigs Ann. Chem.* **1966**, *699*, 24–32. (b) Doering, W. v. E.; X. Zhao, X. *J. Am. Chem. Soc.* **2006**, *128*, 9080–9085.
28. (a) Dewar, M. J. S.; Merz, K. M.; Stewart, J. J. P *J. Chem. Soc., Chem. Commun.* **1985**, 166–168. (b) Liu, Y. P.; Lynch, G. C.; Truong, T. N.; Lu, D. H.; Truhlar, D. G.; Garrett, B. C. *J. Am. Chem. Soc.* **1993**, *115*, 2408–2415. (c) Shelton, G. R.; Hrovat, D. A.; Borden, W. T. *J. Am. Chem. Soc.* **2007**, *129*, 164–168. (d) Kryvohuz, M.; Marcus, R. A. *J. Chem. Phys.* **2012,** 13, 134107-1–13. (e) Edyta M. Greer, E. M.; Kwon, K.; Greer, A.; Doubleday, C. *Tetrahedron* **2016**, *72*, 7357–7373.
29. We thank one of the Reviewers for suggesting this alternative route to aldehyde **7**-H.
30. (a) For decay of **1**-H at 253.2 K, first order rate constants k (mean ± stddev) were $5.62\times10^{-4} \pm 1.8\times10^{-5}$ and $5.25\times10^{-4} \pm 1.2\times10^{-5}$ s^{-1} in acetone-h_6 and acetone-d_6, respectively. For **1**-D at 295.2 K, the corresponding k were $8.46\times10^{-5} \pm 9\times10^{-7}$ and $8.21\times10^{-5} \pm 4.5\times10^{-6}$ s^{-1}. (b) For decay of **1**-H in acetone at 253.2 K, first order rate constants k (mean ± stddev) were $5.62\times10^{-4} \pm 1.8\times10^{-5}$ and $4.93\times10^{-4} \pm 1.9\times10^{-5}$ s^{-1} without and with t-BuN=O dimer (Tables S5A, S6A, Figures S10, S11A & B, SI).
31. (a) Chalfont, G. R.; Perkins, M. J.; Horsfield, A. *J. Am. Chem. Soc.* **1968**, *90*, 7141–7142. (b) Davies, M. J. *Methods* **2016**, *109*, 21–30. (c) Spin concentration of **11**-H is about 7% of the initial spin concentration of **1**-H. (d) One of the lowest energy conformations of **11a**-H has a_N = 1.21 mT at the UB3LYP/6-31G(d,p)/IEF-PCM-UFF + ZPVE level (in acetone) (Table S17, SI).
32. Frisch, M. J. *et al. Gaussian 09*, Revision E.01, Gaussian, Inc., Wallingford CT, **2009**.
33. At the UM06-2X/6-311+G(d,p)/IEF-PCM-UFF + ZPVE level (in acetone), 1,5-HAT had E_a = 21.9 kcal mol^{-1} and **1a**-C1 was 2.5 kcal mol^{-1} above **1a** (Table S16, SI).
34. Eckart, C. *Phys. Rev.* **1930**, 35, 1303–1309. (b) Brown, R. L. *J. Res. Nat. Bur. Stand.* **1981**, *86*, 357–359.
35. We thank one of the Reviewers for very preliminary computations on a simple model molecule (**1a** without t-Bu groups and diethyl ether moiety), using small curvature tunneling, a multi-dimensional approach in Polyrate program, in conjunction with UB3LYP/6-31G(d,p) method in the gas phase. The results indicate that the decay to the corresponding C-radical occurs almost exclusively by tunneling even at room temperature for both D_2-isotopomer (24 times faster by tunneling than by a classical mechanism) and H_2-isotopomer (170 times faster). The computed E_a's for the H_2-isotopomer are 7.7 and 9.5 kcal mol^{-1} at 200 and 300 K, and for D_2-isotopomer 8.7 and 11.8 kcal mol^{-1}. The KIE is 33 at room temperature and 79 at 225 K.

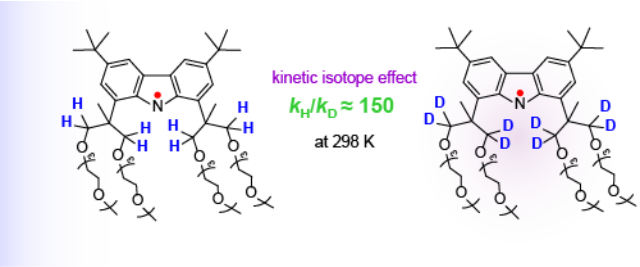
kinetic isotope effect
$k_H/k_D \approx 150$
at 298 K